Taylor & Francis
Taylor & Francis Group

BRIEF REPORT

OPEN ACCESS

Check for updates

Stem cell-like T cell depletion in the recurrent head and neck cancer immune microenvironment

Linda Chen[a], Nancy Lee[a], Reith Sarkar[a], Nora Katabi[b], Yanyun Li[b], Luc Morris[c], Richard Wong[c], Eric Sherman[d], Jorge S. Reis-Filho[b,e], Travis Hollmann[b‡], and Nadeem Riaz[a‡]

[a]Department of Radiation Oncology, Memorial Sloan Kettering Cancer Center, New York, NY, United States; [b]Department of Pathology, Memorial Sloan Kettering Cancer Center, New York, NY, United States; [c]Department of Surgery, Memorial Sloan Kettering Cancer Center, New York, NY, United States; [d]Department of Medicine, Memorial Sloan Kettering Cancer Center, New York, NY, United States; [e]Human Oncology and Pathogenesis Program, Memorial Sloan Kettering Cancer Center, New York, NY, United States

ABSTRACT

Human papilloma virus (HPV)-related oncogenesis in head and neck cancer establishes a local microenvironment rich with immune cells, however the composition of the microenvironment in recurrent disease following definitive treatment is poorly understood. Here, we investigate the composition and spatial relationships between tumor and immune cells in recurrent head and neck cancer following curative intent chemoradiotherapy. Multiplexed immunofluorescence with 12 unique markers, through two multiplex immunofluorescent panels, was performed to evaluate 27 tumor samples including 18 pre-treatment primary and 9 paired recurrent tumors. Tumor and immune cell populations were phenotyped and quantified using a previously validated semi-automated digital pathology platform for cell segmentation. Spatial analysis was conducted by evaluating immune cells within the tumor, peri-tumoral stroma, and distant stroma. Initial tumors in patients with subsequent recurrence were found to be enriched in tumor associated macrophages and displayed an immune excluded spatial distribution. Recurrent tumors after chemoradiation were hypo-inflamed, with a statistically significant reduction in the recently identified stem-like TCF1+ CD8 T-cells, which normally function to maintain HPV-specific immune responses in the setting of chronic antigen exposure. Our findings indicate that the tumor microenvironment of recurrent HPV-related head and neck cancers displays a reduction in stem-like T cells, consistent with an immune microenvironment with a reduced ability to mount T-cell-driven anti-tumor immune responses.

Background

Head and neck squamous cell carcinomas (HNSCC) caused by the human papilloma virus (HPV) are rising in incidence and are associated with excellent long-term survival rates after definitive therapy.[1] HPV status is routinely assessed, and locoregionally advanced HNSCC is often treated non-surgically with a combination of chemotherapy and radiation therapy. Although outcomes in HPV-positive HNSCC are improved in comparison to non-HPV-associated disease, nearly 25% of patients with HPV-related disease still develop recurrence, and the median survival for these patients is only 2.6 years following disease progression.[2] Thus, while there are numerous prospective trials investigating HPV-related HNSCC chemoradiation de-escalation, research focused on recurrent diseases is needed.[3,4] HPV-positive HNSCC has distinct molecular and microenvironmental characteristics from HPV-negative HNSCC, however how the tumor immune microenvironment (TIME) evolves during disease progression remains poorly understood.[5]

Immune evasion plays an important role in oncogenesis for HPV-related HNSCC.[4] In the primary setting, an increased number of lymphocytes in the TIME are thought to contribute to a favorable prognosis in HPV-related disease.[6] Spatial evaluation of immune infiltrates has demonstrated that HNSCC cluster into lymphoid-inflamed, hypo-inflamed, and myeloid-inflamed cancers – with HPV-related cancers clustering with lymphoid inflamed tumors.[7,8] The pro-tumorigenic microenvironment, however, leads to immune-suppression and T-cell exhaustion, though the extent this occurs in recurrent disease requires further elucidation.

Although tumor progression often results in increased immune dysfunction, there are limited human studies evaluating immune cell populations in serially collected tumor samples.[9] Recent profiling of human tumors with single cell (sc) RNA-seq has begun to more clearly differentiate T-cell states from exhausted and effector T-cells, to include a stem-like progenitor population.[10] These stem-like T-cells express TCF1, a transcription factor encoded by the TCF7 gene, known

---

to play an important role in T-cell development. In the setting of chronic viral infection, recent work has identified a subset of virus-specific stem-like CD8+ T cells that retain their potential to proliferate after PD-1 blockade and this subset is dependent on the transcription factor TCF1.[11] These TCF1+CD8+ T cells are thought to represent an adaptation to chronic antigenic stimulation that allows for sustained immune response.[12] Stem-like TCF1+ CD8+ T cells retain proliferative capacity as well as the potential to produce differentiated effectors cells in spite of displaying hallmarks of an "exhausted" phenotype such as PD-1 receptor expression.[13–15] In the current study, we spatially profiled the composition of immune cells within the recurrent TIME and evaluated for the presence of these stem-like TCF1+ CD8+ T cells following an initial course of chemoradiotherapy.

Methods

Patient cohort

Formalin-fixed paraffin embedded (FFPE) tumor samples were obtained from 18 patients diagnosed with HPV-related HNSCC treated at our institution with chemoradiation, half of whom recurred and half of whom are disease free (Supplementary Table S1). Tumor samples were analyzed as part of a Memorial Sloan Kettering Cancer Center institutional review board approved biospecimen protocol IRB #17–103. For the nine patients who developed a recurrence, matched recurrent tumor samples were also analyzed. Adequate tumor specimens for sectioning and staining required a core biopsy at a minimum. HPV status was determined through p16 (antibody clone E6H4 Roche) immunohistochemical staining using the Ventana BenchMark System per manufacturer's protocol. Cases were considered HPV-positive if p16 staining was diffuse and involved greater than 70% of cancer cells. All patients were staged with a PET/CT scan to confirm loco-regionally confined disease before the start of therapy. The data that support the findings of this study are available from the corresponding author (N.R.) upon reasonable request.

Multiplexed immunofluorescence

Hematoxylin and eosin (H&E)-stained slides were reviewed, and FFPE blocks with representative tumor were selected by a pathologist (N.K.). Tumor area for analysis was also identified and annotated by a pathologist on representative H&E slides (N.K.). Embedded tissue was cut as 4 μm sections onto Bond Plus slides. Two panels of seven-color multiplex staining were performed after primary antibodies optimal concentration, and stripping condition were selected by MSK pathologist (T.H.) according to the results of diaminobenzidine immunohistochemical expression on the Leica Bond RX Stainer with Leica Bond Polymer Refine Detection kit (DS9800, Supplementary Figure S1). Four-micrometer thick FFPE tissue sections were baked for 3 h at 62°C upright with subsequent deparaffinization performed on Leica Bond RX,

followed by 30 min of antigen retrieval with Leica Bond ER2, followed by six sequential cycles of staining, each round of which included a 10-min blocking (Akoya antibody diluent/block ARD1001) and 30-min primary antibody incubation (Supplementary Table S2). The primary antibody detection was performed using HRP conjugated species-specific secondary antibody polymer (Supplementary Table S2) with 10-min incubation. The HRP-conjugated secondary antibody polymer was detected using fluorescent tyramide signal amplification using Opal dyes 520, 540, 570, 620, 650, and 690 accordingly (Supplementary Table S2). After each staining cycle, a heat induced stripping of the primary/secondary antibody complex using Akoya AR9 buffer (AR900250ML) and Leica Bond ER2 (90% AR9 and 10% ER2) at 100°C for 20 min preceding the next cycle with Ki67 requiring two sequential rounds of antibody stripping (40 min total). After six sequential rounds of staining, sections were stained with Hoechst (Invitrogen 33,342) to visualize nuclei and mounted with ProLong Gold antifade reagent mounting medium (Invitrogen P36930).

Multispectral imaging and spectral unmixing

Seven-color multiplex-stained slides were imaged using the Vectra Multispectral Imaging System version 3 (Akoya). Scanning was performed at 20X (200X final magnification). Filter cubes used for multispectral imaging were DAPI, FITC, Cy3, Texas Red, and Cy5. A spectral library containing the emitted spectral peaks of the fluorophores in this study was built with the Vectra image analysis software Inform 2.4 (Akoya) using multispectral images from single-stained slides for each marker, the spectral library was used to separate each multispectral cube into individual components (spectral unmixing) allowing for identification of the seven marker channels of interest in the Inform 2.4 image analysis software. The images were exported to the Indica Labs Halo image analysis platform.

Quantitative image analysis

Multispectral fluorescence imaging was acquired on a Vectra Polaris automated imaging system. A minimum of five representative regions of interest (ROI), with each ROI measuring approximately 1.3×1 mm^2, were selected by a blinded laboratory technician within the pathologist annotated tumor regions. Tumor and immune cell populations were phenotyped and quantified using semi-automated cell segmentation with the Halo digital pathology platform. Signal thresholding was performed separately on each image. Spatial analysis was conducted using the HALO proximity and infiltration analysis, to determine the number of cells of interest within the tumor, peri-tumoral stroma (100 μm from the tumor/stroma interface), and distant stroma (>100 μm). A mixing score previously published by Keren et al. was used to quantify cellular spatial relationships and was calculated by measuring tumor and immune cell interactions[16]. The mixing score was calculated by dividing the number of tumors and immune cells within 15 μm by the number of immune cells with 15 μm of another immune cell. Two-sided Student's t-test was used for statistical

analysis between initial tumors that remained disease-free vs. initial tumors which recurred after definitive chemoradiation. PD-L1 combined positive score (CPS) was defined as the number of PD-L1 positive cells (tumor cells, lymphocytes, and macrophages) divided by the total number of tumor cells. Wilcoxon signed-rank test for matched pairs was used for statistical analysis between matched primary and recurrent tumors. Graphical and statistical analyses were performed in GraphPad Prism version 6.0.

The Cancer Genome Atlas (TCGA) analysis

RNA sequencing gene expression transcripts per million (TPM) data for TCF7 and CD8A were imported from the TCGA RNA sequencing head-neck squamous cell carcinoma (HNSC) and cervical squamous cell carcinoma and endocervical adenocarcinoma (CESC) datasets using the GDCquery function of the TCGAbiolinks R-package.[17–20] For patients with CESC, only those with squamous cell carcinoma were analyzed. Survival data for the HNSC and CESC datasets were obtained from data provided by Liu et al.[21] For the HNSC group, patients were categorized by HPV status (positive vs. negative) and for both the HNSC and CESC groups were dichotomized according to the median expression values of TCF7 and CD8A gene expression. Additionally, patients were grouped by combined TCF7 and CD8A count: TCF7 high and CD8A high, TCF7 high and CD8 low, TCF7 low and CD8 high, TCF7 low and CD8 low. Kaplan–Meier curves for the overall survival and progression-free intervals were generated using the survival and ggplot packages in R. Cox proportional hazards models were generated using the survival and gtsummary packages in R.

Results

Pre-treatment recurrent tumors are enriched in tumor associated macrophages and are immune compartmentalized

We identified 18 patients with HPV-related oropharyngeal malignancies (located in the tonsil or base of tongue), including nine patients who developed recurrence. All patients were treated with definitive concurrent chemoradiation (Supplementary Table S1). The standard of care treatment consisted of concurrent cisplatin or carboplatin/5-fluorouracil-based chemotherapy with intensity-modulated radiation therapy. The FFPE tissue was obtained for analysis, and tissue was evaluated from the primary tumor for $n = 21$ tumors and from a cervical lymph node in $n = 6$ samples (Supplementary Table S1). Patients had AJCC 7th edition staging of T1-T3 N0-N2c disease. The median follow-up was 39.7 months (range 11.6–78.7 months), and the time to locoregional failure was a median of 7.8 months (range: 5.2–25 months).

We first evaluated the density of immune infiltrates (CD3+ T-lymphocytes, CD68+ tumor-associated macrophages, and CD20+ B lymphocytes) in pre-treatment initial tumors that remained disease free after therapy vs. initial tumors that
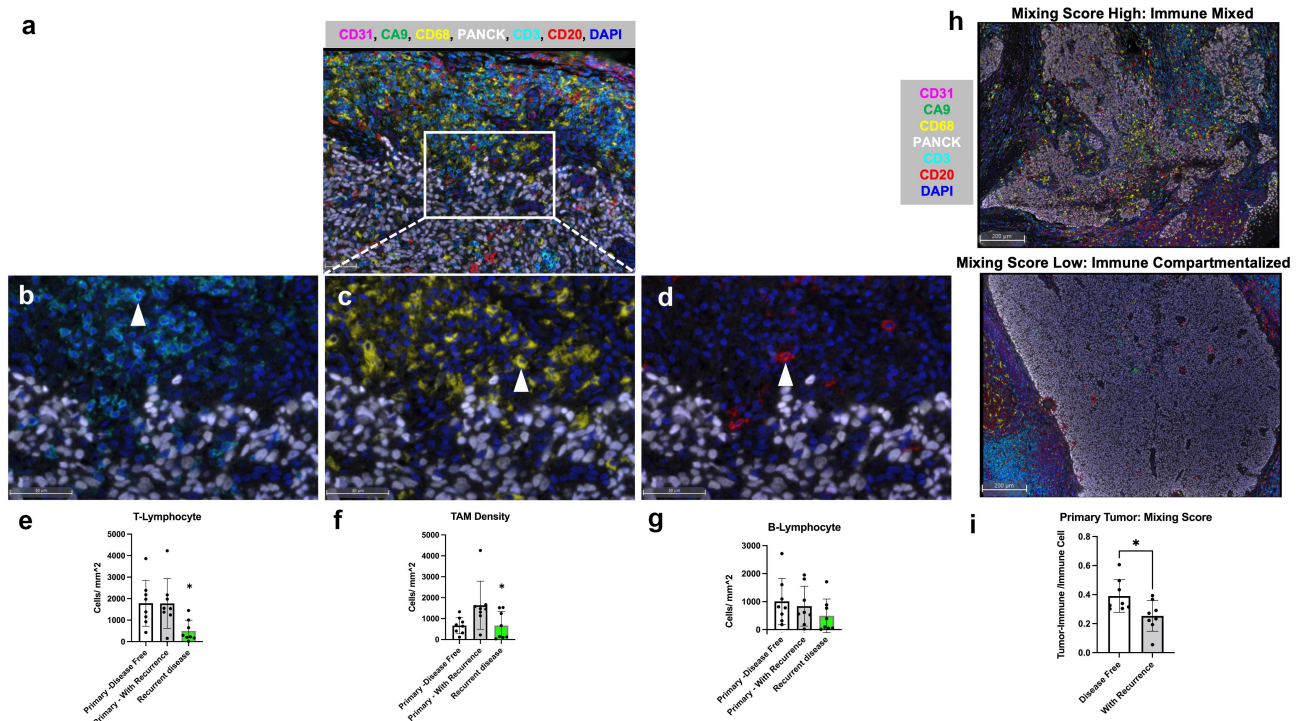

Figure 1. Immune composition of pre-treatment initial tumors (DF – initial) which remain disease free, initial tumors which developed recurrence, (R – initial), and recurrent tumors. a. Multiplexed immunofluorescent staining of CD31 (magenta), CA9 (green), CD68 (yellow), PanCK (white), CD3 (teal), CD20 (red), and DAPI (Blue) at 20× magnification. b. CD3+ T-lymphocyte at 40×. c. CD3- CD68+ (yellow) tumor associated macrophage at 40×. d. CD20+ (red) B lymphocyte at 40×. e-g: T-lymphocyte ($p = 0.007$), tumor associated macrophage ($p = 0.025$), and B-lymphocyte density in primary tumors with and without disease recurrence. h. Representative examples of mixing score high (immune mixed) and mixing score low (immune compartmentalized) tumors at 10× magnification. i: Primary tumor mixing score with and without disease recurrence ($p = 0.010$).

recurred after treatment (Figure 1). Patients who recurred after chemoradiation had pre-treatment tumors that were enriched with tumor-associated macrophages (CD3−, CD68+, $p = 0.025$), with a mean density of 1637 cells/mm^2 in primary tumors which subsequently recurred, compared to 670 cells/mm^2 in pre-treatment tumors that remained disease free following treatment. In this cohort, the density of CD3+ T-lymphocytes and CD20+ B-lymphocytes was not significantly different between pre-treatment initial tumors that did or did not recur after chemoradiation.

We next sought to investigate the spatial relationships between neoplastic and immune cells using a previously described mixing score (*see Methods*). Briefly, this score quantifies tumor-immune cell interactions and differentiates between tumors that had high levels of intermixed immune infiltrate and those with compartmentalized immune infiltrate. We found that pre-treatment initial tumors that did not recur had a significantly higher mixing score compared to pre-treatment tumors that recurred. Pre-treatment recurrent tumor was characterized by more immune compartmentalization (mean mixing score 0.390 vs. 0.253, respectively, $p = 0.0104$).

Post-treatment recurrent tumors are hypo-inflamed & depleted of stem like TCF1+ T-cells

We next focused our attention on the evolution of the immune micro-environment in tumors that recurred. In this cohort of matched ($n = 9$ pairs) pre-treatment initial tumors and post-treatment recurrent tumors, we evaluated the density of immune infiltrates (Figure 1). Following definitive chemoradiation, recurrent tumors had significantly reduced density (cells/mm^2 of immune infiltrate with fewer T-lymphocytes (CD3+, CD68−, $p = 0.007$) and macrophages (CD3−, CD68+, $p = 0.027$). There was no statistically significant change in B cells (CD3−, CD20+). These results are consistent with a generally less immune infiltrated TIME during cancer recurrence.[22]

We next evaluated specific T-cell populations in matched ($n = 9$ pairs) pre-treatment primary tumors and post-treatment recurrent tumors (Figure 2b). We sought to understand whether the global decrease in (CD8+) T cells was driven by a specific sub-population or was independent of T cell state. Surprisingly, there was no increase in the percentage of exhausted (CD8+, PD1, EOMES+/CD8+) T cells nor was there a decrease in the percentage of proliferating T-cells (Ki67+ CD8+/CD8+) at time of recurrence compared to pre-treatment. At the time of recurrence, however, there was a statistically significant reduction in the percentage of stem-like T-cells (TCF1+, CD8+/CD8+ T cells, $p = 0.039$).

These TCF1+ T cells in our study are located predominantly within the stroma, with a depletion of intra-tumoral TCF1+ T cells in recurrent tumors. Specifically, pre-treatment TCF1+ T-cells were 21.6% intra-tumoral, 48.6% peri-tumoral stroma (i.e. up to 100 μm from tumor-stroma interface), and 29.8% within the distant stroma. Recurrent tumors had a statistically significant reduction in the percentage of intra-tumor TCF1+ T-cells (6.6%, $p = 0.012$), with a relative concomitant increase in the percentage of TCF1+ T-cells located in the peri-tumoral stroma and stroma (Figure 2c).

Finally, we evaluated PD-L1 positivity in tumor and immune cells. %PD-L1 tumor cells ranged from 0% to 93%, median 15% and there was no statistically significant difference between the initial tumors and those that remained disease free or recurred (Supp Figure S1). There was also no statistically
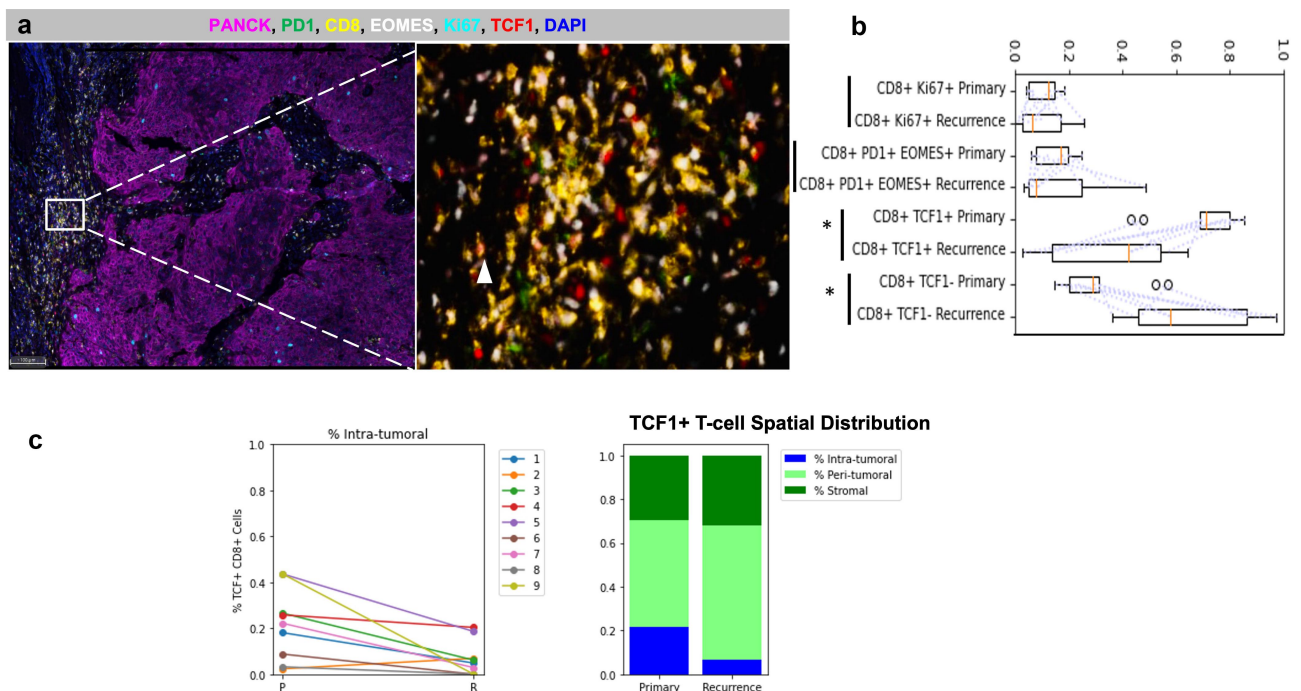

Figure 2. Depletion of TCF1+ CD8+ lymphocytes. a. 63× magnification of stem-like T cell (TCF1+ CD8+) staining. b. Percent of CD8 T cells which are: proliferating T-cells (CD8+ Ki67+), exhausted T cells (CD8+ PD1+ EOMES+), and stem-like T cells (CD8+ TCF1+) in matched initial and recurrent tumors. c. Percent intra-tumoral, peri-tumoral (within 100 microns of tumor–stroma interface, $p = 0.012$), and stromal TCF1+ CD8+ T cells in matched primary and recurrent tumors.

significant difference between paired initial and recurrent tumors. PD-L1 CPS ranged from 1% to 100%, with a median of 29%. CPS was also not statistically significantly different between groups.

Transcriptomic analysis of TCF expression in HPV associated malignancies

To investigate the prognostic importance of TCF1+ T-cells in a broader context, we evaluated the correlation between TCF expression in two HPV-related cancers, head and neck and cervical cancer (CESC, Figure 3). Kaplan–Meier estimates of the overall survival for CESC dichotomized with high vs. low TCF7 expression by the median TPM value (5.47) and demonstrated that patients with low TCF7 expression were associated with significantly worse overall survival (HR 1.91, 95% CI: 1.14–3.22, $p = 0.015$). In HNSC, we first noted that TCF7 expression was higher in HPV-related malignancy vs. HPV-negative HNSCC (median TPM 7.0 vs 3.3, $p < 0.001$). Kaplan–Meier estimates of the overall survival for HPV+ HNSCC patients with high vs. low TCF7 expression, dichotomized by the median TPM value (3.61), revealed numerically worse overall survival in cancers with low TCF7 expression (HR 1.78, 95% CI 0.68–4.71, $p = 0.2$), although this was not statistically significant.

Discussion

HPV-positive HNSCC have a distinct immune profile, with divergent T, B, and myeloid cell transcriptional profiles compared to the HPV-negative cancers.[23] This immune profile is prognostic, and even within HPV-positive disease, the presence of a high density of tumor infiltrating T cells is associated with improved survival.[24] Furthermore, the TIME plays an important role in response to chemo-radiotherapy, and we sought to evaluate how the TIME evolves in treatment resistant HPV-positive tumors.

Here we analyze changes in the TIME within paired pre- and post-treatment recurrent HPV-associated HNSCCs following chemoradiation and demonstrate that following a course of curative intent therapy, recurrent tumors are hypo-inflamed. We report the novel observation of a preferential reduction of progenitor T cells, which are TCF1+, CD8+ T cells, in post-therapy recurrent samples. These TCF1+ T-cells are located predominantly within the stroma, and we demonstrate a significant reduction in the proportion of intra-tumoral TCF1+ T cells in recurrent tumors. Furthermore, transcriptional TCGA and survival analysis from HPV+ HNSC as well as CESC patients suggest that TCF7 expression may be prognostic.

Limited data exist on specific T-cell subset composition at the time of recurrence due to difficulty in acquiring paired patient samples of sufficient quality. Stem-like T-cells are of particular interest in HPV-related cancers as they play an important role in oncogenesis. TCF7 expressing stem-like CD8 T cells play a crucial role in maintaining T cell responses to persistent antigen exposure and have the capacity to differentiate into HPV-specific effector-like T cells.[25]

In addition to this, the capacity of stem-like cells to proliferate significantly influences responses to anti-PD1-based therapies.[11,22,25] Recent work has demonstrated that these stem-like cells frequently inhabit specific clusters of immune cells within tumors.[26] Moreover, it has been found that exhausted T-cells in tumors can often be traced back, or
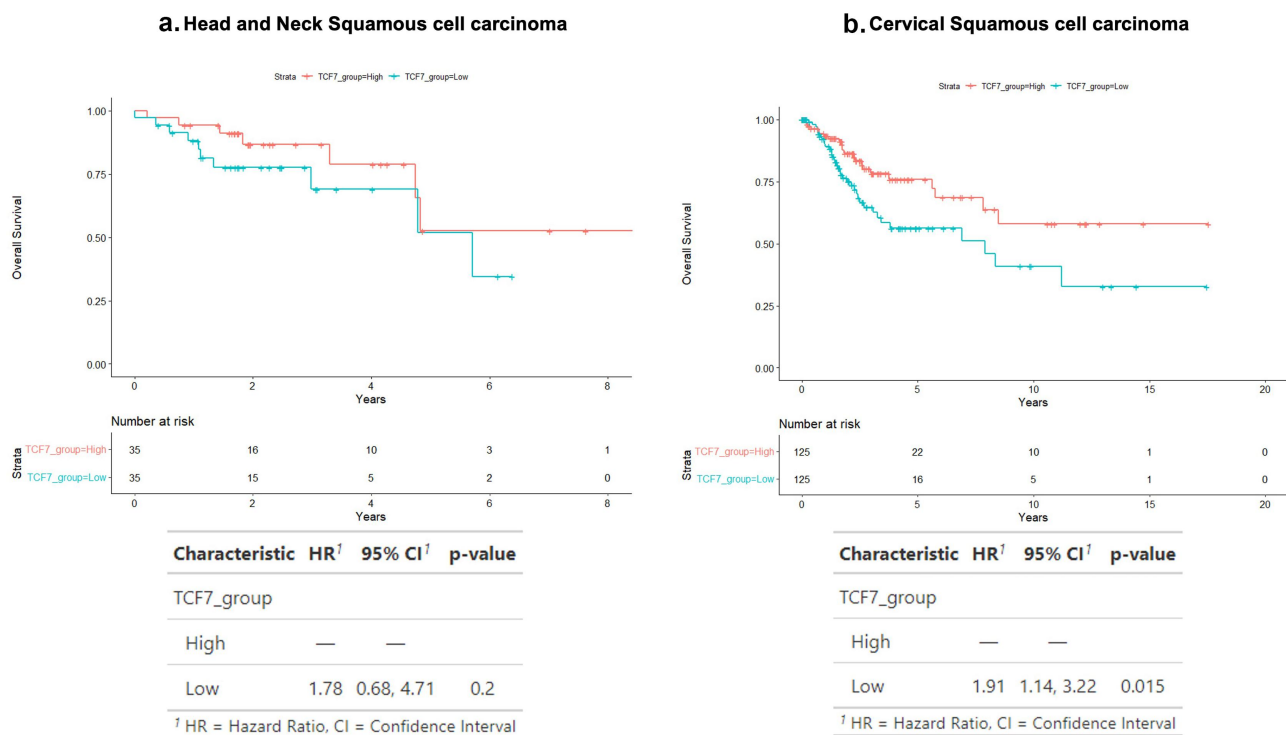

Figure 3. Overall survival of a) HPV+ Head and neck squamous cell carcinoma and b) Cervical squamous cell carcinoma dichotomized by median TCF7 transcriptional expression.

'clonally linked', to these stem-like cells located in tumor draining lymph nodes. To our knowledge, the role of stem-like T-cells and radiotherapy's effects on them in mediating the recent failures of immunotherapy combined concurrently with conventionally fractionated chemoradiation in HNSCC patients (i.e. JAVELIN, HN004, and KEYNOTE-412) remain unknown. Given our observation of decreases in stem-like T-cells in patients who recur after radiotherapy, this will clearly be an important future direction.

Yet, it is unclear whether the reduction in this subset of T-cells is only found in the setting of chemoradiation or if it is a characteristic of recurrent cancers that have established a more pro-tumorigenic TIME with less potential for an anti-tumor immune response.[27,28] Interestingly, though, in Keynote-048, which tested pembrolizumab in recurrent/metastatic HNSCC, there was no significant benefit of pembrolizumab in locally recurrent disease, which could suggest therapy-induced changes in TIME may influence efficacy of subsequent therapy.[29] Therefore, our findings warrant further studies assessing the predictive impact of the observed TIME changes in HNSCC patients treated primarily with solely surgical approaches vs those who recur after chemo-radiotherapy.

Finally, we compared pre-treatment tumors in patients who remained disease free vs. pre-treatment tumors which subsequently recurred and did not find a significant difference in CD3+ T-cell or CD20+ B-cell infiltration, likely due to limited patient numbers. A significant difference in the spatial distribution of tumor and immune cells was observed, where initial tumors that recur were found to display a significantly more compartmentalized immune infiltrate. We also noted a significant increase in CD3–CD68+ tumor-associated macrophages, which is consistent with previously published data that report that a subset of poor prognostic HPV-positive tumors harbor myeloid-inflamed profiles.

This study has several limitations including a relatively small sample size ($n = 18$ patients) and our findings require validation in future cohorts of paired cases. This reflects the challenges in obtaining representative tissue in paired pre- and post-therapy in patients treated with chemoradiation that is amenable to multiplex immunophenotyping in HPV-related disease, which recurs infrequently after chemoradiation. Second, sequencing data were not available for our patient cohort, and genetic heterogeneity with respect to driver mutations may confound our findings. Additionally, our evaluation of the prognostic value of TCF expression in HNSCC was acquired from bulk RNA-sequencing and demonstrated a prognostic trend that was not statistically significant. Further evaluation of whether TCF1+ T-cell population in the TIME is prognostic requires multiplex immunophenotyping of larger samples size of recurrent and non-recurrent tumors. Despite these limitations, we provide a novel characterization of the immune TME changes in recurrent post-treatment samples of HNSCC.

In summary, we provide a novel characterization of the TIME changes in recurrent post-treatment samples of HNSCC patients. We identify that recurrent tumors are more likely to be enriched in macrophages at the time of initial diagnosis and become hypo-inflamed with depletion of stem-like T-cells at the time of recurrence. Stem-like T-cells play an important role in anti-PD1-based therapies, and these data provide early evidence of their role in locoregional recurrence in a clinical population.[11,22]

References

1. Ang KK, Harris J, Wheeler R, Weber R, Rosenthal DI, Nguyen-Tân PF, Westra WH, Chung CH, Jordan RC, Lu C, et al. Human papillomavirus and survival of patients with oropharyngeal cancer. New Engl J Medicine. 2010;363(1):24–35. doi:10.1056/NEJMoa0912217.
2. Fakhry C, Psyrri A, Chaturvedi A. HPV and head and neck cancers: state-of-the-science. Oral Oncol. 2014;50(5):353–355. doi:10.1016/j.oraloncology.2014.03.010.
3. Orlandi E, Iacovelli NA, Tombolini V, Rancati T, Polimeni A, De Cecco L, Valdagni R, De Felice F. Potential role of microbiome in oncogenesis, outcome prediction and therapeutic targeting for head and neck cancer. Oral Oncol. 2019;99:104453. doi:10.1016/j.oraloncology.2019.104453.
4. Bird T, De Felice F, Michaelidou A, Thavaraj S, Jeannon J-P, Lyons A, Oakley R, Simo R, Lei M, Guerrero Urbano T, et al. Outcomes of intensity-modulated radiotherapy as primary treatment for oropharyngeal squamous cell carcinoma – a European single institution analysis. Clin Otolaryngol. 2017;42(1):115–122. doi:10.1111/coa.12674.
5. Lawrence MS. Comprehensive genomic characterization of head and neck squamous cell carcinomas. Nature. 2015;517:576–582.

6. Ward MJ, Thirdborough SM, Mellows T, Riley C, Harris S, Suchak K, Webb A, Hampton C, Patel NN, Randall CJ, et al. Tumour-infiltrating lymphocytes predict for outcome in HPV-positive oropharyngeal cancer. Brit J Cancer. 2014;110 (2):489–500. doi:10.1038/bjc.2013.639.

7. Tsujikawa T, Kumar S, Borkar RN, Azimi V, Thibault G, Chang YH, Balter A, Kawashima R, Choe G, Sauer D, et al. Quantitative multiplex immunohistochemistry reveals myeloid-inflamed tumor-immune complexity associated with poor prognosis. Cell Rep. 2017;19 (1):203–217. doi:10.1016/j.celrep.2017.03.037.

8. Brooks JM, Menezes AN, Ibrahim M, Archer L, Lal N, Bagnall CJ, von Zeidler SV, Valentine HR, Spruce RJ, Batis N, et al. Development and validation of a combined hypoxia and immune prognostic classifier for head and neck cancer. Clin Cancer Res. 2019;25(17):5315–5328. doi:10.1158/1078-0432.CCR-18-3314.

9. Philip M, Schietinger A. CD8+ T cell differentiation and dysfunction in cancer. Nat Rev Immunol. 2022;22(4):209–223. doi:10.1038/s41577-021-00574-3.

10. Blank CU, Haining WN, Held W, Hogan PG, Kallies A, Lugli E, Lynn RC, Philip M, Rao A, Restifo NP, et al. Defining 'T cell exhaustion'. Nat Rev Immunol. 2019;19(11):665–674. doi:10.1038/s41577-019-0221-9.

11. Bhatt KH, Neller MA, Srihari S, Crooks P, Lekieffre L, Aftab BT, Liu H, Smith C, Kenny L, Porceddu S, et al. Profiling HPV-16–specific T cell responses reveals broad antigen reactivities in oropharyngeal cancer patients. J Exp Med. 2020;217(10):e20200389. doi:10.1084/jem.20200389.

12. Im SJ, Hashimoto M, Gerner MY, Lee J, Kissick HT, Burger MC, Shan Q, Hale JS, Lee J, Nasti TH, et al. Defining CD8+ T cells that provide the proliferative burst after PD-1 therapy. Nature. 2016;537(7620):417–421. doi:10.1038/nature19330.

13. Jadhav RR, Im SJ, Hu B, Hashimoto M, Li P, Lin J-X, Leonard WJ, Greenleaf WJ, Ahmed R, Goronzy JJ, et al. Epigenetic signature of PD-1+ TCF1+ CD8 T cells that act as resource cells during chronic viral infection and respond to PD-1 blockade. Proc Natl Acad Sci USA. 2019;116(28):14113–14118. doi:10.1073/pnas.1903520116.

14. Zander R, Schauder D, Xin G, Nguyen C, Wu X, Zajac A, Cui W. CD4 + T cell help is required for the formation of a cytolytic CD8+ T cell subset that protects against chronic infection and cancer. Immunity. 2019;51(6):1028–1042.e4. doi:10.1016/j.immuni.2019.10.009.

15. Hudson WH, Gensheimer J, Hashimoto M, Wieland A, Valanparambil RM, Li P, Lin J-X, Konieczny BT, Im SJ, Freeman GJ, et al. Proliferating transitory T cells with an effector-like transcriptional signature emerge from PD-1+ Stem-like CD8+ T cells during chronic infection. Immunity. 2019;51(6):1043–1058.e4. doi:10.1016/j.immuni.2019.11.002.

16. Keren L, Bosse M, Marquez D, Angoshtari R, Jain S, Varma S, Yang SR, Kurian A, Van Valen D, West R, et al. A structured tumor-immune microenvironment in triple negative breast cancer revealed by multiplexed ion beam imaging. Cell. 2018;174(6):1373–1387.e19. doi:10.1016/j.cell.2018.08.039.

17. Colaprico A, Silva TC, Olsen C, Garofano L, Cava C, Garolini D, Sabedot TS, Malta TM, Pagnotta SM, Castiglioni I, et al. Tcgabiolinks: an R/Bioconductor package for integrative analysis of TCGA data. Nucleic Acids Res. 2015;44(8):e71. doi:10.1093/nar/gkv1507.

18. Therneau TM (2022) A package for survival analysis in R. https://cran.r-project.org/web/packages/survival/index.html.

19. Wickham H, Chang W, Henry L, Pedersen TL, Takahashi K, Wilke C, Woo K, Yutani H, Dunnington D Create elegant data visualisations using the grammar of graphics • ggplot2. https://ggplot2.tidyverse.org/.

20. Sjoberg DD, Whiting K, Curry M, Lavery JA, Larmarange J. Reproducible summary tables with the gtsummary package. R J. 2021;13(1):570–580. doi:10.32614/RJ-2021-053.

21. Liu J, Lichtenberg T, Hoadley KA, Poisson LM, Lazar AJ, Cherniack AD, Kovatich AJ, Benz CC, Levine DA, Lee AV, et al. An integrated TCGA pan-cancer clinical data resource to drive high-quality survival outcome analytics. Cell. 2018;173(2):400–416. e11. doi:10.1016/j.cell.2018.02.052.

22. Gonzalez H, Hagerling C, Werb Z. Roles of the immune system in cancer: from tumor initiation to metastatic progression. Gene Dev. 2018;32(19–20):1267–1284. doi:10.1101/gad.314617.118.

23. Cillo AR, Kürten CHL, Tabib T, Qi Z, Onkar S, Wang T, Liu A, Duvvuri U, Kim S, Soose RJ, et al. Immune landscape of viral- and carcinogen-driven head and neck cancer. Immunity. 2020;52 (1):183–199.e9. doi:10.1016/j.immuni.2019.11.014.

24. Ward MJ, Thirdborough SM, Mellows T, Riley C, Harris S, Suchak K, Webb A, Hampton C, Patel NN, Randall CJ, et al. Tumour-infiltrating lymphocytes predict for outcome in HPV-positive oropharyngeal cancer. Br J Cancer. 2014;110 (2):489–500. doi:10.1038/bjc.2013.639.

25. Eberhardt CS, Kissick HT, Patel MR, Cardenas MA, Prokhnevska N, Obeng RC, Nasti TH, Griffith CC, Im SJ, Wang X, et al. Functional HPV-specific PD-1+ stem-like CD8 T cells in head and neck cancer. Nature. 2021;597(7875):279–284. doi:10.1038/s41586-021-03862-z.

26. Chen JH, et al. Spatial analysis of human lung cancer reveals organized immune hubs enriched for stem-like CD8 T cells and associated with immunotherapy response. bioRxiv 2023 04 04 535379. 2023. doi:10.1101/2023.04.04.535379

27. Sade-Feldman M, Yizhak K, Bjorgaard SL, Ray JP, de Boer CG, Jenkins RW, Lieb DJ, Chen JH, Frederick DT, Barzily-Rokni M, et al. Defining T cell states associated with response to checkpoint immunotherapy in Melanoma. Cell. 2019;176(1–2):404. doi:10.1016/j.cell.2018.12.034.

28. Brummelman J, Mazza EMC, Alvisi G, Colombo FS, Grilli A, Mikulak J, Mavilio D, Alloisio M, Ferrari F, Lopci E, et al. High-dimensional single cell analysis identifies stem-like cytotoxic CD8+ T cells infiltrating human tumors. J Exp Med. 2018;215 (10):2520–2535. doi:10.1084/jem.20180684.

29. Burtness B, Harrington KJ, Greil R, Soulières D, Tahara M, de Castro G, Psyrri A, Basté N, Neupane P, Bratland Å, et al. Pembrolizumab alone or with chemotherapy versus cetuximab with chemotherapy for recurrent or metastatic squamous cell carcinoma of the head and neck (KEYNOTE-048): a randomised, open-label, phase 3 study. Lancet. 2019;394(10212):1915–1928. doi:10.1016/S0140-6736(19)32591-7.